Analysis of Performance Degradation of Silica Gels after Extended Use Onboard the ISS

Gregory E. Cmarik[1]
Jacobs Space Exploration Group, Huntsville, AL, 35812

James C. Knox[2] and Timothy L. Huff[3]
NASA/Marshall Space Flight Center, Huntsville, AL, 35812

The disassembly of two flight desiccant beds from the Carbon Dioxide Removal Assembly (CDRA) revealed significant discoloration of the silica gel near the bed inlet as well as a coincidental performance loss. This material was analyzed for the presence of chemical contaminants, physical porosity changes, and adsorption performance. The material characteristics are compared against the location in the bed from which they were sampled in order to develop profiles through the bed. Additional testing of the beds prior to disassembly provided more data points. Possible mechanisms for the loss of capacity are provided though no root cause has been confirmed. Extrapolation of the performance loss is used to estimate the required oversizing of the silica gel layer for long-term operation.

Nomenclature

ISS	=	International Space Station
CDRA	=	Carbon Dioxide Removal Assembly
4BMS	=	4-Bed Molecular Sieve
POIST	=	Performance & Operations Issues System Testbed
SG40	=	Sylobead® SG 40 (Grade 40)
SGB125	=	Sylobead® SG B 125 (SGB125)
DAB	=	Desiccant-Adsorbent Bed
GC-MS	=	Gas Chromatography – Mass Spectrometry
ICP-AES	=	Inductively Coupled Plasma – Atomic Emission Spectroscopy
BET	=	Brunauer, Emmett, and Teller method
MSFC	=	Marshall Space Flight Center
ECLSS	=	Environmental Control and Life Support Systems
CDRA4-EU	=	Carbon Dioxide Removal Assembly – 4 Engineering Unit
TGA	=	Thermogravimetric Analysis/Analyzer
MFC	=	Mass Flow Controller
4BMS-X	=	4-Bed Molecular Sieve for Exploration (test stand)
DSC	=	Differential Scanning Calorimetry
HC	=	Half-Cycle
D3-D6	=	Silicon-Oxygen (Si-O) Siloxanes with 3 to 6 Cyclic Si-O Functional Groups

I.   Introduction

ONBOARD the International Space Station (ISS) one of the CO_2 removal systems is the Carbon Dioxide Removal Assembly (CDRA). CDRA is a flight-qualified 4-bed molecular sieve (4BMS) system which uses desiccant beds which contain silica gel as the bulk drying material. Upon return from orbit, the silica gel used in the desiccant beds for the CDRA system were found to be significantly altered from original. This alteration was found to be three-fold: a readily visible translucent orange hue for a previously clear and colorless material, adsorption of

---

[1]ECLSS Engineer, Jacobs Space Exploration Group, Marshall Space Flight Center/ES62.
[2]Chemical Engineer, NASA, Marshall Space Flight Center/ES62.
[3]Material Scientist, NASA, Marshall Space Flight Center/EM22.

various low vapor pressure trace contaminants found throughout the ISS cabin atmosphere, and, most importantly, reduced desiccant performance. This paper summarizes the efforts conducted to characterize the material changes and also predict whether it will have any negative impact on the performance of a system during a long-duration mission.

Anecdotal past experiences have shown this discoloration to be present in both on-ground and in-orbit materials, though not in all tests. The Performance & Operations Issues System Testbed (POIST) test series in 2003 was run for extensive amounts of time and showed a similar discoloration, with photos of flight and POIST bed teardowns provided in Figure 1. Other flight bed disassembly procedures have found similar discoloration but samples were not made available for study. During the time where CDRA-3 beds were in use on station, siloxanes were identified as a major concern for atmospheric contamination. The effect of siloxanes was significant on other systems on the ISS,[1] therefore it was decided to study the silica gels which are most directly exposed to ISS cabin air contaminants.

Two commercially available silica gels have been used as the bulk desiccant in the various CDRA iterations. Both materials were manufactured by Grace-Davison and are known as Silica Gel Grade 40 (SG40) and Silica Gel B125 (SGB125). SG40 is a granular material while SGB125 is a beaded material with superior structural resilience and virtually identical adsorption performance versus SG40.

At the time of this report, two pairs of desiccant beds have been disassembled and sampled for further study. To date, fifteen desiccant beds have been flown as part of Desiccant-Adsorbent Bed (DAB) units. Several studies on the samples from first pair of flight desiccant beds were conducted in 2013-2015.[2] This also resulted in the first set of flight samples being severely depleted. Gas Chromatography – Mass Spectrometry (GC-MS) analysis identified numerous components, particularly siloxanes D3-D6, to be present in the samples from the end of the bed closest to the cabin air inlet/outlet. Inductively Coupled Plasma – Atomic Emission Spectroscopy (ICP-AES) analysis identified compositional changes throughout the bed.
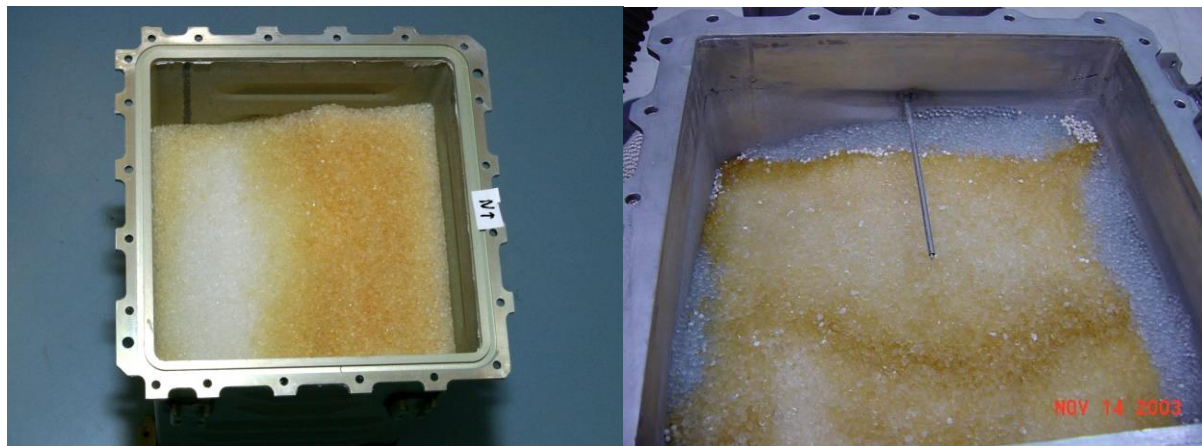

Figure 1: Photos of desiccant bed disassembly for flight (left) and POIST (right) showing discoloration of silica gel. Samples are removed layer-by-layer with a vacuum transfer line enabling sample collection at specific depths.

From these data points, a need to study the next available flight desiccant beds was identified. Test plans were developed to replicate the previous studies and determine new factors. In addition to GC-MS and ICP-AES analysis, Brunauer, Emmett, and Teller (BET) analysis and newly developed water vapor adsorption analyses would be conducted. Flight DABs from the CDRA-4 were returned in 2015 for disassembly and study.

II.   Test Procedures and Test History

Analyses conducted by the Materials Test Lab at Marshall Space Flight Center (MSFC) include: GC-MS, ICP-AES, and BET method adsorption. These tests follow standard procedures established by the Materials Test Lab. Adsorption tests conducted by the Environmental Control and Life Support Systems (ECLSS) branch at MSFC were designed for this test series.

After return from flight but before bed disassembly, the first test was conducted on the desiccant bed D0003. This first test was conducted in three parts. First, the desiccant bed was installed in CDRA-4 Engineering Unit (CDRA-4EU) and tested with the improved instrumentation available at MSFC to determine if early water breakthrough occurs. Second, the bed was thoroughly dried in an oven up to 175°C. Finally, the bed was
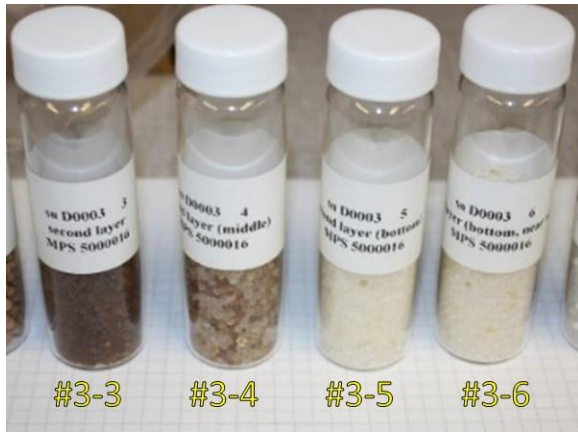
Figure 2: Photo of silica gel samples from CDRA-4 flight desiccant bed D0003. Sample -3 is from the end nearest the cabin air inlet and -6 is from the end adjacent the 13X layer.

challenged with a 10°C dew point air stream for an extended period of time. After this test, the unit was dried and returned for disassembly. Disassembly was conducted via layer-by-layer removal of material with a vacuum hose. At specified depths (0", 2", 4", 5.5"), the removed material was recovered for testing. The silica gel samples from D0003 are shown in Figure 2.

The samples recovered from desiccant beds D0003 and D0004 from CDRA-4 were tested for water vapor adsorption performance. A SETARAM *Sensys Evo* Thermogravimetric Analyzer (TGA) with a *Wetsys* water vapor generator, an auxiliary Mass Flow Controller (MFC), and a LICOR *LI-840a* CO_2/H_2O gas analyzer were used to control and monitor the gas composition, temperature, and sample mass. Samples were activated at 50°C to mimic past testing,[2] which dried samples at 45°C, with the reasoning that an activation temperature above nominal CDRA operation would potentially drive off adsorbed contaminants and alter the results. Samples are very small, typically 2 beads per measurement.

III. Results and Discussion

A. Chemical Analysis

Chemical composition analysis results from the CDRA-3 samples showed a correlation between siloxane content and loss of performance.[2] Other correlations were noted between excess metal content and performance loss. The chemical composition analysis results from the CDRA-4 samples shows no correlation between siloxane nor metal content and loss of performance. There was no detectable siloxane content on all of the CDRA-4 samples except for a small amount on the Sorbead WS material sourced from D0003. Reports[3, 4] indicate that a fraction of adsorbed siloxanes will be irreversibly adsorbed but nothing to explain the complete lack of detectable siloxanes. It is possible that the adsorbed siloxanes would be lost to evaporation and permeation over time as this was observed in duplicate testing of CDRA-3 samples. The metal content was very consistent across the entire depth of bed D0003. As will be shown later, the adsorption performance strongly varies with sample depth, therefore any assumption of primary causation between sorbent degradation and siloxane and/or metal content must be reduced to a secondary or correlating factor.

B. Porosity Analysis

Surface area and pore volume analysis via the BET method showed a consistent trend across sample depth. The BET method utilizes N_2 adsorption at 77K and enables study of the surface area, micropore volume, total pore volume, pore size distribution, and a number of other porosity properties. Figure 3 shows a summary of the properties for samples from D0004 compared with control samples. Surface area losses of up to 35%
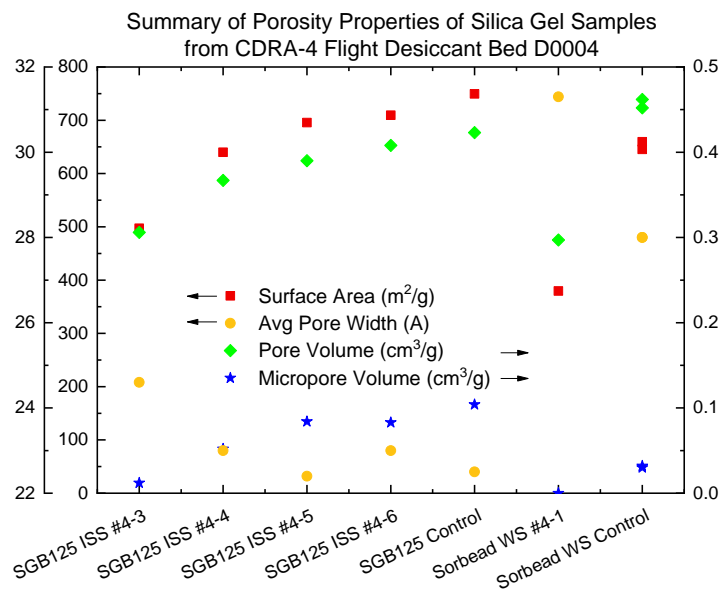
Figure 3: Summary of porosity properties for a series of control samples and samples from desiccant bed D0004 used in CDRA-4.

International Conference on Environmental Systems
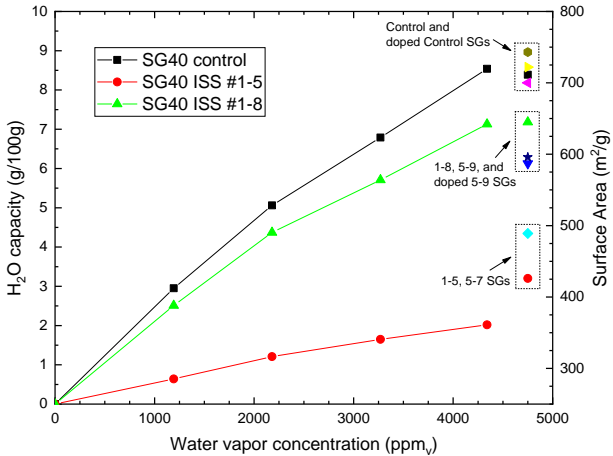
Figure 4: Results of testing on samples of control and the remaining flight SG40 as well as all available past surface area analyses of the various samples.

are measured which is slightly less severe than the 45% loss measured for some samples from CDRA-3. Surface area correlates with adsorption performance in virtually any situation, including this study. Pore volume correlates with total capacity which occurs when pores completely fill with sorbate molecules. Average pore width and micropore volume provide additional information on the size and shape of the pores. Surface area, pore volume, and micropore volume are found to increase and show a positive correlation with adsorption capacity. Average pore width is roughly equal for all samples except for the sample from the front of the bed which was larger. A conclusion from this set of data is that the interconnected network of pores are altered in a manner that yields fewer pores and skews the structure towards more macropores. Two mechanisms are likely to cause these observations. First, blocked pores cause a reduction in pore volume and thus the total adsorption capacity will be reduced. Second, the surface area and micropore volume are reduced resulting in reduced adsorption performance at low partial pressures.

C. Water Vapor Adsorption at 25°C – Low Concentration (up to -2°C dew point)

Based on previous reports,[2] initial testing was directed at the effects of adsorbed contaminants in the material. Therefore, low concentration isotherms were measured where adsorption should occur via layering on the surfaces of the pores. This is as opposed to a pore filling mechanism, where water vapor condenses as a continuous liquid phase within the pore chambers at high concentrations. Therefore, any measured uptake of water vapor should correlate to the availability and affinity of the pore surfaces for water. Should hydrophobic contaminants, such as siloxanes, be present as a surface monolayer within the pore structure then a marked reduction should be observed due to the reduced affinity whereas N_2 surface analysis should not show a major difference. If both water and N_2 capacity are reduced, then it is possible that contaminants fill the porous network extensively or, alternatively, the porous structure could be compromised.

In Figure 4, the first iteration of testing on the two remaining flight SG40 samples was compared with unused SG40 and SGB125 from drums kept in storage on the ground. Measured surface areas are included to aid visibility of the correlation. The results in the previous report[2] indicated a severe degradation of material performance and showed a correlation to both presence of contaminants and reduction in surface area. Initial results shown in this study support those correlations. A definitive conclusion could not be reached with the limited test material remaining from the CDRA-3 flight beds D0001 and D0005.

The flight desiccant beds used in CDRA-4 were returned and sampled. A slightly altered procedure was developed to test this series of SGB125 flight and control samples with the results shown in Figure 5. The results from porosity analysis and chemical analysis indicate
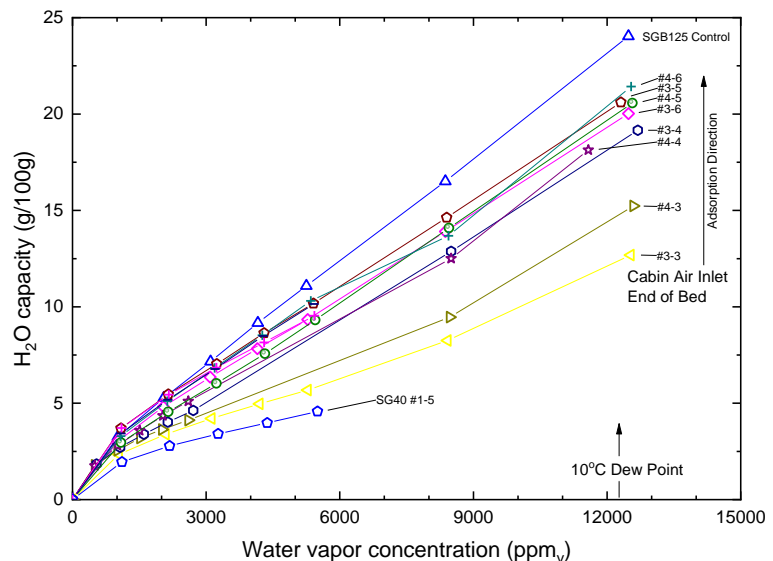
Figure 5: Water vapor isotherms obtained for control and flight silica gel samples at 25°C. For reference, the adsorbing flow direction of CDRA vs sample depth is shown for correlation to sample capacity.
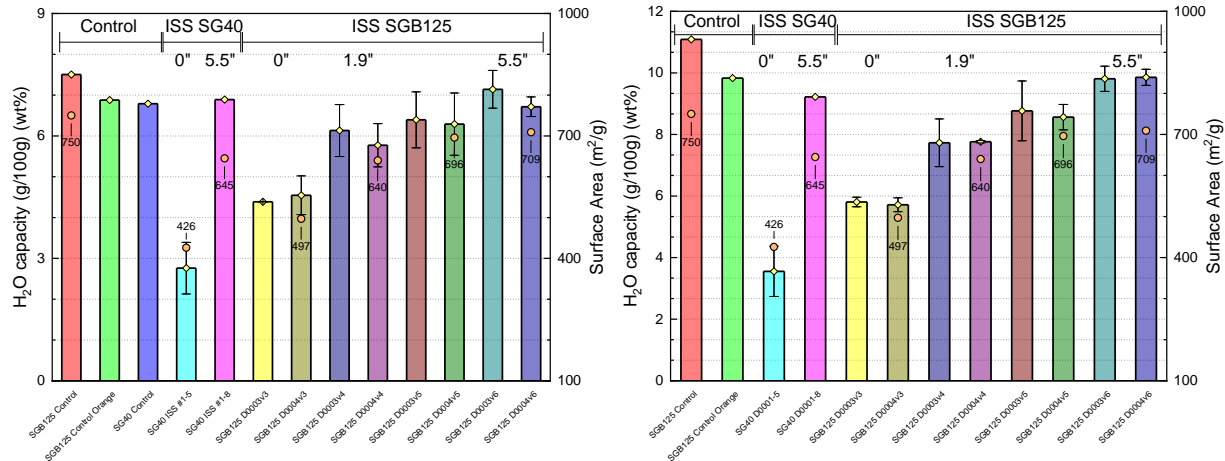
Figure 6: Results of water vapor adsorption test at low concentrations. Adsorption was conducted at 25°C and interpolated at 3250 [left] and 5250 [right] ppmv water vapor.

that the best correlation to loss of water capacity is loss of porosity. This could indicate that a physical pore closing process is responsible for the performance loss. Since no recoverable siloxanes were observed in the CDRA-4 samples, a contaminant coating of the surface can be discounted. The measurements of remaining CDRA-3 materials correlate a reduction of surface area by 45% results to a nearly 70% water capacity loss as shown by the difference between control and #1-5 samples. The CDRA-4 sample measurements for the #3-3 and #4-3 samples show a 35% reduced surface area and a 50% capacity loss. One major caveat is that the #1-5 sample had a selection bias due to only three remaining granules.

The water vapor isotherms shown previously are reduced to two particular water vapor concentrations for easier comparison in the form of a column chart. Since the data points were not collected at exactly the same concentrations, values were normalized to 3250 and 5250 ppm by assuming a linear relationship between concentration and capacity. The shape of the isotherms justify this method. Since each sample was tested at least twice, the results are reduced to mean and span values for each sample. Finally, sampling depths from bed disassembly notes and surface area data are included to generate the plots shown in Figure 6. Four orange-tinted beads were observed near the surface in the source drum of SGB125. These were individually extracted and tested with the results identified as "control orange."

The trends are more readily visible in this format. Surface area correlates strongly with capacity. The samples taken from the end of the desiccant bed closest to the cabin air inlet show the greatest loss of performance, while samples taken from positions that correspond to drier sections of the bed which also see hotter temperatures are more similar to control samples. All flight samples show at least a slight reduction in performance versus control samples.

D. Water Vapor Adsorption at 25°C – High Concentration (up to 10°C dew point)

To affirm the working theory that the cause of performance loss is loss of surface area, a study of the materials at water vapor levels equivalent to 10°C dew point at 25°C sample temperature was conducted. At the time of these measurements, neither lower sample temperatures nor higher dew points could be obtained. The normalized capacity values are shown in Figure 7 along with corresponding surface areas as reference. The additional isotherm points are shown in Figure 5
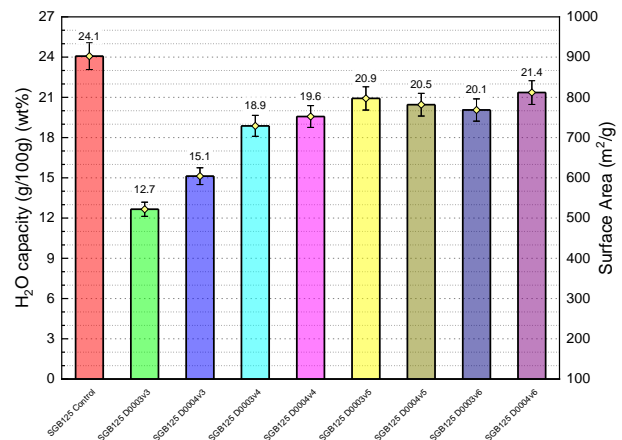
Figure 7: Results of one water vapor adsorption test designed to match the inlet concentration for CDRA. Adsorption was conducted at 25°C and interpolated at 12,500 ppmv.

and are connected with the previously obtained isotherms. A nearly linear extrapolation from lower water vapor concentration results is observed. The samples from the front of the bed is severely degraded by almost 50% from the control sample while the remainder of the bed shows a 15% to 25% reduction in capacity. This performance loss may be significant to system operation as the front of the bed adsorbs a large fraction of water during each cycle.

These isotherms do not show a distinct plateau at high concentrations, which would indicate complete saturation of the pores, thus no correlation can be made between total pore volume and total capacity. Recently, efforts have revealed that pore saturation only occurs when dew point is nearly equal to sample temperature, a condition approaching 100% relative humidity, which cannot be tested in the TGA.
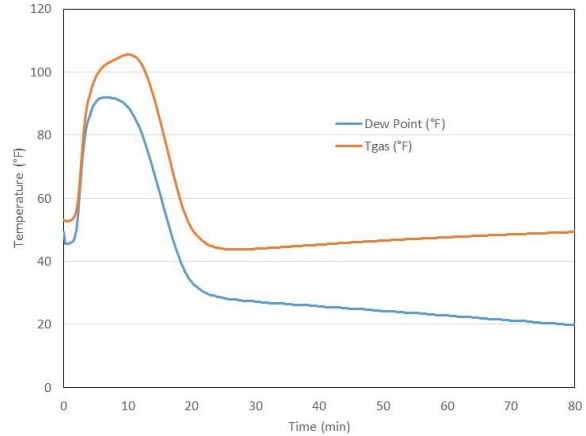

Figure 8: COMSOL simulation of the 4BMS system in operation showing the air temperature and dew point at the inlet of the silica gel layer of the desiccant bed during a desorption cycle. The two traces overlap indicating a condition of 100% RH.

E. Computer simulation of CDRA operation

An ongoing effort to accurately model the complex dynamics of a cyclic CO_2 removal system may be able to provide some insight. During desorption cycles of a desiccant bed, a water vapor concentration wave and a hot temperature wave are observed. The hot purge drives desorption by providing the endothermic desorption process with heat. Ahead of the hot purge a cold region develops due to some desorption occurring into the dry gas. These thermal and concentration waves progress through the bed at different rates with the concentration wave preceding the hot purge wave.

There may be a point where the cool, water-laden wave leads to a condition of 100% relative humidity. Contact of silica gel with liquid water is known to cause the silica gel to fracture. The computer simulation does indicate a condition of 100% RH within the silica gel layer near the cabin air inlet end as shown in Figure 8. This 100% RH condition occurs within the first third of the bed as bounded by sample depths that showed the most degradation (D3-3 to D3-4 and D4-3 to D4-4). Perhaps this unique condition is a contributor to the silica gel degradation.

F. Test Data from 4BMS Operation

In addition to computer simulations of the next generation system, a full-scale test stand (4BMS-X test stand) is being used to validate against existing system behaviors and test new conditions. Data from one of the most recent test series is shown in Figure 9. Anecdotal observation of droplets of water at the system outlet has occurred on
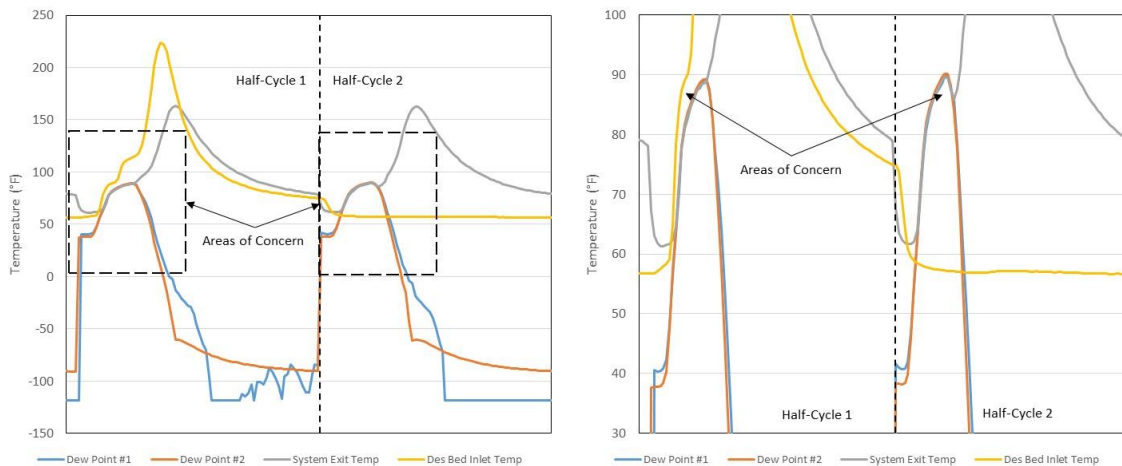
Figure 9: 4BMS-X test data (4Xr3-61) showing the temperature at the inlet of one desiccant bed and the system outlet along with two independent dew point measurements of the system outlet. Of particular note is the overlap of temperature and dew point curves at the early parts of a desorption cycle.

many occasions during operation of this system. The data gathered during desorption of a number of test series show the exit dew point nearly parallel with a temperature probe (labelled desiccant bed inlet) embedded at a point that would be equivalent to a bed depth between flight samples 3 and 4.

Despite hundreds of half-cycles of operation, these desiccant beds did not have observable silica gel discoloration nor observable particle fracturing when beds were disassembled and emptied. No record of the exact number of half-cycles of operation presently exists. A procedural bed teardown and depth sampling was not required and therefore did not occur.
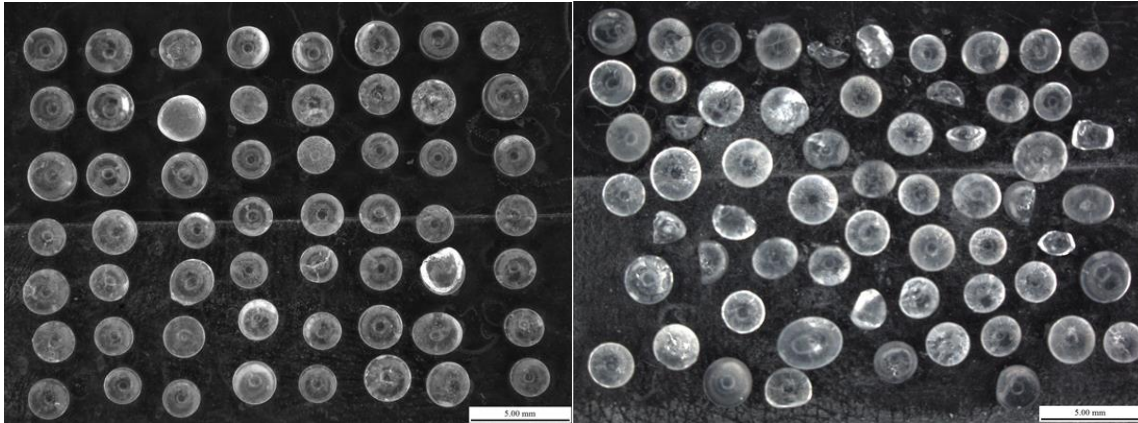

Figure 10: Photos of SGB125 from misting test report. Before [left] and after [right] misting.

G. Silica Gel Misting

Based on manufacturer notes, SGB125 and SG40 particles break when exposed to liquid water. This is a well-known behavior of silica gel across industry and is the reason for the protective Sorbead WS layer. An internal test to quantify misting-induced degradation was conducted and reported in 2015 by an ECLSS summer intern. Silica gel samples were conditioned with water vapor at 10°C dew point at ambient temperature then sprayed with a fine mist of liquid water. The results of that work was that silica gel beads fracture and show a slight loss of capacity (~2%). Figure 10 shows the broken SGB125 samples from this test. Since the test was conducted only once per sample, perhaps the effects on internal structure become measurable only after repeated exposure and cycling.

No broken silica gel beads were mentioned in flight bed disassembly notes, perhaps due to the difficulty in observing them. A small number of broken silica gel beads were found in the D3v3 and D4v3 vials but were only observed due to the small sample vials. Pictures of these broken beads are shown in Figure 11 and the pattern of breakage is similar to the misting test with the major exception of orange discoloration. One hypothesis that can be
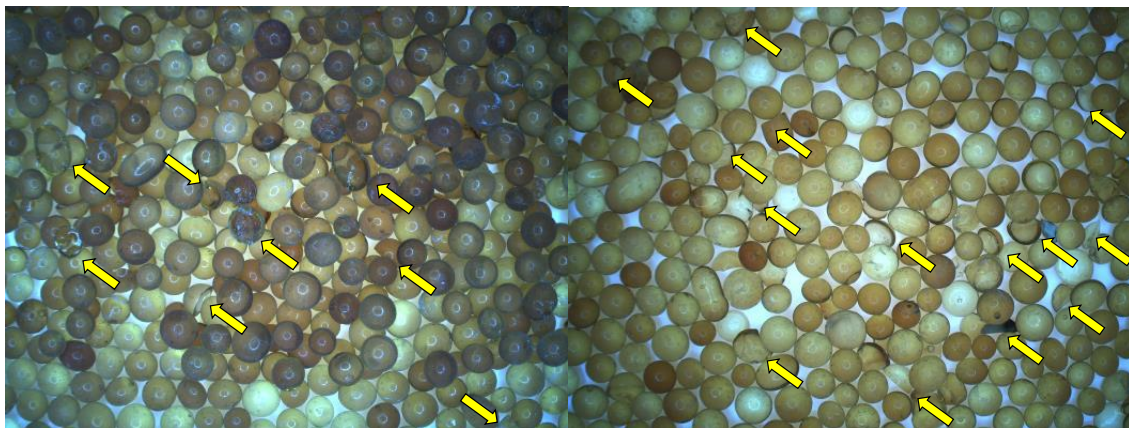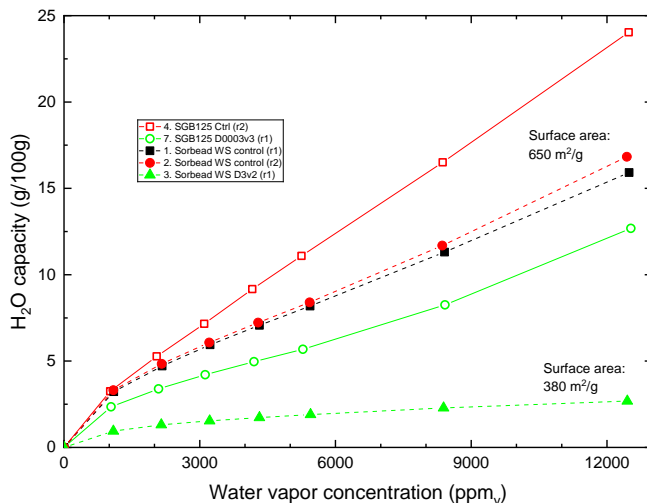

Figure 11: Photos of SGB125 sampled from the inlet of both CDRA-4 desiccant beds with arrows indicating some of the broken silica gel particles intermixed with the bulk.

made is that the concentration wave poses a significant stress on the silica gel particles during each desorption cycle, sometimes to an extent similar to misting, and may be a cause of performance loss.

H. Water Vapor Adsorption – Sorbead WS

Both water vapor adsorption tests were conducted on the vials of desiccant that was sampled from the guard layer. The guard layer is 1" deep and composed of BASF Sorbead WS, a misting-stable silica gel with high robustness but reduced desiccation performance. The guard layer is the first sorbent layer exposed to incoming air and thus is expected to be most severely affected by possible contaminants. If misting occurs from upstream systems, the Sorbead WS will capture the liquid droplets and guard the bulk desiccant. The BET surface area for control samples is $650 m^2/g$ but only $380 m^2/g$ for flight sample #4-1. The same water vapor isotherms were measured on these samples. The results in Figure 12 clearly show an extensive

Figure 12: Water adsorption isotherm on two silica gels, SGB125 (solid lines) and Sorbead WS (dashed lines). Control and flight samples are shown along with the surface area measurements for the respective samples of Sorbead WS.

loss in performance (~85%). This is extremely surprising considering the primary criterion for this material's selection was robustness. This observation indicates the mechanism which imparts particle robustness is different from the mechanism for pore stability.

I. Water Vapor Adsorption – Zeolite 13X

Another water vapor isotherm measurement procedure was developed to study the performance of the 13X zeolite used in the flight desiccant beds. This material is commercially available as MS544 from Grace-Davison. At the MSFC test facility there are a number of lots of material available for testing, though not the same as the flight lot. The results in Figure 13 show that the material sampled from flight bed D0004 is indistinguishable from available control samples across a wide range of adsorption temperatures. New capabilities enabled simultaneous DSC operation in the *Sensys Evo* TGA which provides the data to calculate heat of adsorption. This new data is shown as well and correlates with widely published heats of adsorption for 13X in the range of 70-80 kJ/mol. The spread of the data points can be attributed to the derived nature of these values.
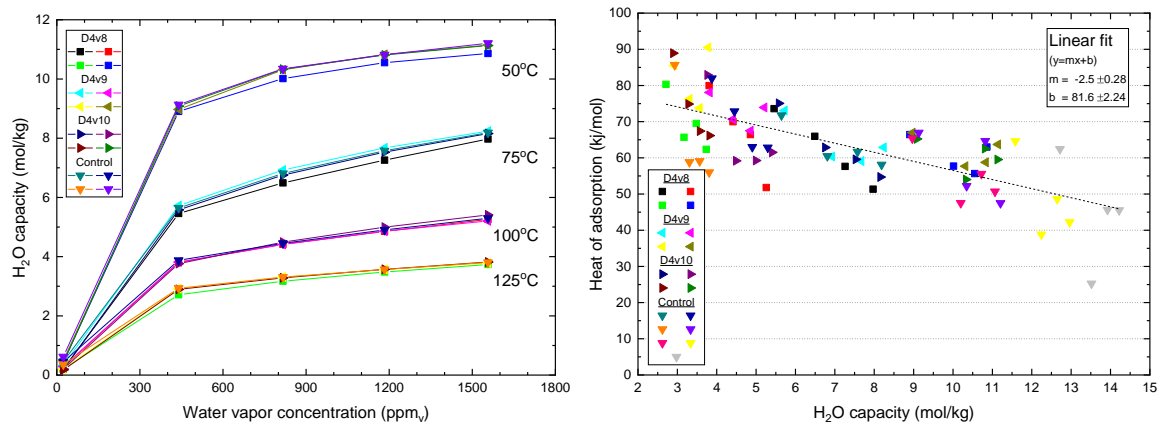
Figure 13: Water adsorption isotherms [left] and heat of adsorption [right] measurements on control and D0004 flight samples of zeolite 13X showing the seemingly imperturbable performance of the material.

J. Bed Oversizing Estimates

The overall goal of studying flight samples and analyzing this data is to generate a prediction for desiccant bed lifetimes and sizing. There will be 19,723 half-cycles during a 3 year mission with 80 minute half-cycles. The working theory is that only the desorbing half-cycle generates the conditions that lead to silica gel degradation, thus there will be 9862 desorption half-cycles. A basis of 10,000 half-cycles will be used for estimates. The estimates for bed lifetime are extrapolations due to insufficient data. Additionally, no CDRA bed has operated for 3 years or in excess of 6,000 half-cycles (3,000 desorbing half-cycles).

1. Estimate from average bed performance

The first estimate is based on the reduced initial breakthrough time of CDRA-4 D0003 versus the CDRA-4EU beds DevW and DevS.[5] This data is sourced from an internal report on the testing of these three beds after return-from-flight but before disassembly. The data in this report indicated that desiccation performance loss from use in flight had occurred and the breakthrough curves are shown in Figure 14.

Two aspects can be considered, the total capacity and the trace breakthrough time. All beds were challenged with the same inlet condition, therefore breakthrough time is roughly equivalent to performance. The overall capacity for each test is nearly equal as shown in Table 1. On the other hand, the first detectable breakthrough occurs at 64% of the time of the ground-based units. These fractions can be used to estimate a bed size for a 3-year mission. Since these beds must maintain extremely dry gas streams for the CO_2 sorbent and downstream systems, the time when trace water is detected is more critical. What needs to be calculated is the performance loss of the materials that can still ensure complete desiccation for entire half-cycle times after years of use.

Table 1: Desiccant bed capacities for flight bed D0003 and the two development beds used in the 4BMS-X test stand.

	FltD0003	DevS	DevW
Capacity at Trace Breakthrough (lb)	2.11	3.35	3.60
Trace Breakthrough Time (min)	190	297	313
Capacity at 0°F Breakthrough (lb)	4.56	4.68	4.53
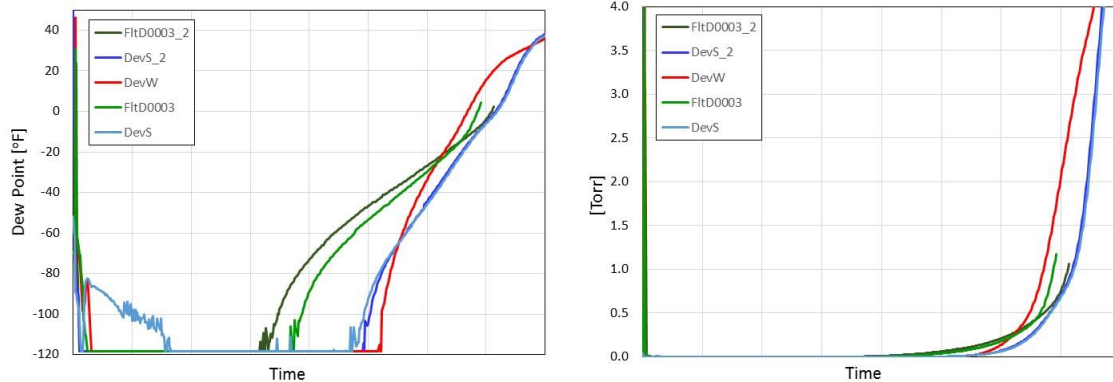
Figure 14: Results from the flight and development bed breakthrough tests. Dew point [left] is highly non-linear enhancing the visibility of trace breakthrough while the identical plot in partial pressure [right] shows the similarity of total capacity. The early trace breakthrough of flight bed D0003 is clearly visible in the left plot.

At CDRA inlet conditions of 12°C and 10°C dew point, silica gel adsorbs water up to 38% by weight and zeolite 13X adsorbs up to 25% by weight while also requiring significantly more heat to desorb. The beds are roughly 50/50 by volume and silica gel has a roughly 15% higher packing density based on packing masses from Cylindrical Breakthrough Test logs. The assumptions to be made is that silica gel performance loss accounts for the entirety of total capacity reduction, the 13X layer behaves the same for each test, and the capacity of the guard layer is negligible. These assumptions can be justified by the data shown in previous sections. After correcting for small test differences, the expected average silica gel layer capacity of the flight bed would be 61% of the development beds. As a note, the average capacity for the flight samples as a fraction of control sample is 79%, therefore the more strongly degraded end of the bed has a more significant impact on bed performance.

Extrapolations of trace breakthrough time with this assumption yields two data points. The development unit beds are treated as if at 0% performance loss and possess a breakthrough time of 297 minutes. The flight beds are

International Conference on Environmental Systems

set to 39% performance loss and a time of 190 minutes. With only 2 points, a linear extrapolation can be made. The design half-cycle time of the next generation 4BMS system is 80 minutes, which would correlate to initial breakthrough occurring when the silica gel layer capacity drops to 53% of original levels. Since the flight bed operated for 2370 desorbing half-cycles, a linear rate of capacity loss would extrapolate an early breakthrough after 4806 half-cycles. The silica gel layer depth would need to be increased by an additional 108% to sustain a 3-year mission, if all assumptions and estimates are accurate.

For other estimates, the 53% capacity value will be used as a cutoff for silica gel layer performance, below which trace water breakthrough would occur in an 80 minute half-cycle system. Further refinement of this estimate will be approached via detailed computer simulation.

2. Estimate – Different mechanisms for capacity loss are applied to halves of silica gel layer
A second estimate requires assumptions that the inlet half of the silica gel layer is degraded via one mechanism while another mechanism occurs for the second half. The inlet half, characterized by -3 and -4 samples, is degraded by the relative humidity spike previously described. The half closer to the 13X layer, characterized by -5 and -6 samples, is degraded by high temperatures. The high temperature is necessary to regenerate the 13X desiccant and, from POIST and 4BMS-X test data, the temperature of the silica gel reaches a peak of 170°C. It is known that exceedingly high temperatures on the order of 350°C will permanently damage the pore surfaces of silica gel by chemically removing hydrophilic hydroxyl groups.[6] That report also activated silica gel at 200°C under vacuum for 2 hours without noticeable differences from the 120°C activation baseline, although hundreds of cycles are not tested. Overall, the assumptions for this estimate are not flawless but they lead to a simple estimate.

Samples -5 and -6 from both beds show equivalent behavior and on average show 86% of the capacity of control samples. This value is assumed to be the post-thermal degradation capacity for the hotter half of the bed indefinitely. The inlet half of the bed is assumed to degrade at a constant rate each desorbing half-cycle based on the performance loss of -3 and -4 samples. Extrapolating from these assumptions, this set of assumptions essentially means that half of the bed will be nearly at peak performance for an indefinite amount of time and the estimated lifespan is over 37,000 half-cycles. This means the bed size does not need to be increased any further.

IV. Conclusions

Flight desiccant beds returned from use on station have shown a loss of performance. These beds were tested before and after disassembly and compared to engineering unit beds. Samples taken from the flight bed were tested as well as remaining previous flight samples. Characterization of the flight is conducted via chemical, porosity, and adsorption analysis techniques. Chemical contamination was previously proposed as the cause of silica gel degradation but was not found to be a factor in these samples. Porosity and adsorption analysis revealed strong correlations, thus loss of capacity due to physical loss of porosity in the silica gel may be the cause.

A new cause of degradation was proposed and is identified in the normal operation of 4BMS systems. This cause is the desorption of water from the desiccant bed which produces a temporary condition of 100% relative humidity. This condition fully saturates the silica gel and is soon followed by extensive drying. This complete loading and unloading process causes small performance losses and occurs each desorbing half-cycle.

Extrapolations are made with the new data and alternative mechanisms. A threshold for drying failure was defined as time until detectable breakthrough of water vapor and set to 80 minutes to match with the next generation 4BMS system. This was estimated to occur when the silica gel layer of a CDRA-4 desiccant bed was reduced to 53% of original capacity. Two mechanisms are proposed which would either require no additional silica gel to compensate for losses to doubling the present amount of silica gel. Further study via computer simulation is recommended to understand the bed capacity at various extents of silica gel degradation.

V. References

[1]Perry, J. L., and Kayatin, M. J. "The Incidence and Fate of Volatile Methyl Siloxanes in a Crewed Spacecraft Cabin," 2017.

[2]Huff, T., Knox, J. C., Boothe, R., and Bowman, E. "Evaluation of Sorbent Capacity Following Contamination in the ISS Atmosphere," *45th International Conference on Environmental Systems*. Bellevue, Washington, 2015.

[3]Montanari, T., Finocchio, E., Bozzano, I., Garuti, G., Giordano, A., Pistarino, C., and Busca, G. "Purification of landfill biogases from siloxanes by adsorption: A study of silica and 13X zeolite adsorbents on hexamethylcyclotrisiloxane separation," *Chemical Engineering Journal* Vol. 165, No. 3, 2010, pp. 859-863.

[4]Sigot, L., Ducom, G., Benadda, B., and Labouré, C. "Adsorption of octamethylcyclotetrasiloxane on silica gel for biogas purification," *Fuel* Vol. 135, 2014, pp. 205-209.

[5]Peters, W., and Stanley, C. "Breakthrough Test Report," 2016.

[6]Christy, A. A. "Effect of heat on the adsorption properties of silica gel," *International Journal of Engineering and Technology* Vol. 4, No. 4, 2012, p. 484.

VI.   Acknowledgements